

Bi- tri- and few-layer graphene growth by PLD technique using Ni as catalyst

UMBER KALSOOM*, M. SHAHID RAFIQUE, SHAMAILA SHAHZADI, KHIZRA FATIMA, RABIA SHAHEEN

Department of Physics, University of Engineering and Technology, Lahore-54890, Pakistan

The objective of the present research work is to optimize the growth conditions of bi- tri- and few-layer graphene using pulsed laser deposition (PLD) technique. The graphene was grown on n-type silicon (1 0 0) at 530 °C. Raman spectroscopy of the grown films revealed that the growth of low defect tri-layer graphene depended upon Ni content and uniformity of the Ni film. The line profile analysis of the AFM micrographs of the films also confirmed the formation of bi- tri- and a few-layer graphene. The deposited uniform Ni film matrix and carbon/Ni thickness ratio are the controlling factors for the growth of bi- tri- or few- layer graphene using pulsed laser deposition technique.

Keywords: *graphene; Raman spectroscopy; atomic force microscopy; pulsed laser deposition*

1. Introduction

Graphene is being investigated as a building block of graphite since 1940s [1]. In 2004, Novoselov successfully identified graphene layers and its discovery in 2004 completed the carbon family [2]. It is a two-dimensional building block of carbon allotropes and can be stacked into 3D graphite, rolled into 1D nanotube CNT, or wrapped into 0D fullerenes [1, 3]. Variety of different carbon related crystalline and non-crystalline structures may exist in different sp^2 and sp^3 hybridization states [4]. Graphene exhibits unique electronic properties, for instant, high charge carrier mobility and quantum Hall effect [5]. Utilization of all these properties is based on the availability of fine and controllable fabrication technique.

Initially, graphene was formed by micromechanical cleavage [2]. Metals like nickel, platinum and cobalt have also been used in the synthesis of graphene [6–8]. Graphene prepared on a metal substrate possesses more uniform layers due to dissolution and precipitation of carbon in metal [9, 10]. The number of graphene layers depends on how

much carbon atoms segregate from the carbon-metal solid solution [11, 12]. The lattice constants of Si, Ni and C are 0.543 nm, 0.352 nm and 0.332 nm, respectively. A smaller lattice mismatch between Ni and C provides better opportunity to grow graphene layers. Graphene can be grown using several techniques such as micromechanical cleavage [2], thermal decomposition [13] and metal induced graphitization [14, 15] graphite oxide reduction [16], molecular beam epitaxy (MBE) [17], chemical vapor deposition (CVD) [18] and pulsed laser deposition (PLD) [19, 20].

Among these, PLD is well-known to produce graphene from multilayer to few layers [21]. Therefore, it is expected to promote carbon adatom diffusion into Ni film at low substrate temperature. In addition, the thickness ratio of Ni to graphite film can be controlled easily in PLD by varying the number of laser shots on Ni and graphite. Keeping in mind these aspects, controllable growth of graphene can be obtained by PLD technique [22]. In this research work, Ni based bi- tri- and few-layer graphene has been grown on Si substrate using PLD technique.

*E-mail: umber.uet@gmail.com

2. Experimental

In this experiment, bi- tri- and few-layer graphene have been deposited using nickel-graphite (Ni-C) target on n^+ silicon (1 0 0) substrate. Ni was used as a catalyst. The target Ni-C was prepared by embedding Ni disc of ~ 2 cm diameter into the graphite disc of ~ 5.7 cm in diameter. A schematic of the Ni-C target is shown in Fig. 1a. The target was mounted on a target holder fitted with a rotatory motor as well as a translatory motorized stage. The rotatory motor rotated the target during the deposition and the translatory motor brought either graphite or Ni in front of the laser beam. Si substrate was placed in parallel to the multicomponent target at a distance of 1.6 cm.

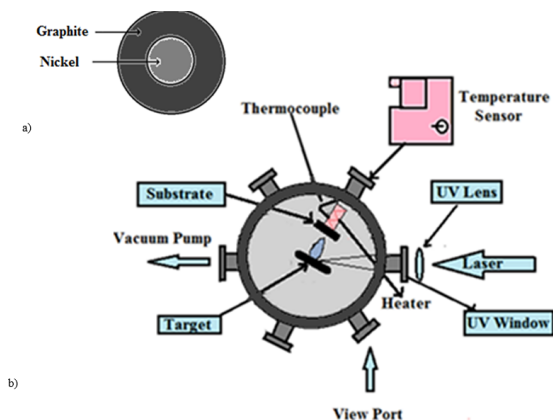


Fig. 1. (a) schematic Ni and graphite disc used as a target, (b) schematic of experimental setup.

Schematic of the experimental setup is shown in Fig. 1b. A KrF excimer laser (248 nm, 20 mJ, 20 Hz), placed at an angle 45° to the target surface was used to ablate the target. The experiment was carried out in a stainless steel chamber evacuated to a pressure of 1.33×10^{-3} Pa by rotary and turbomolecular pumps.

To deposit the graphene films, Ni was deposited at the first step. Immediately after the Ni deposition, the substrate temperature was raised to 530°C in order to enlarge the average grain size of Ni film. Afterwards, graphite was deposited on the Ni layer. The deposited films were allowed to cool down naturally at room temperature under vacuum. Graphene thin films were fabricated by varying

the number of laser shots on Ni part of the target and the number of laser shots on graphite part was kept constant. Five films were deposited under the scheme listed in Table 1.

For the structural analysis, all the as-deposited films were analyzed by HORIBA Jobin Yvon LabRAM HP Raman spectrometer using 632.8 nm laser as the excitation source. Atomic Force Microscopy (AFM) Veeco was used to evaluate the thickness and the number of graphene layers.

3. Results and discussion

3.1. Raman analysis

Raman spectroscopy is the most reliable, non-destructive and quick inspection method to get information of graphene and carbon related structures [4]. Fig. 2 shows Raman spectra of films grown at different Ni concentrations (different number of laser shots on nickel) keeping graphite concentration (number of laser shots on graphite) constant. The spectra exhibit three remarkable peaks (for all Ni concentrations) observed at 1330, 1590 and 2670 cm^{-1} . The Raman peak appearing at 1330 cm^{-1} is referred to as D band. D band originates due to defected graphite and is usually called disorder-induced D band. It is associated with the breathing mode of sp^2 aromatic rings. D band is energy dispersive and a slight shift in its position (if there is any) might depend on the change in the excitation energy [23]. The second prominent Raman peak appearing at 1590 cm^{-1} is referred to as G band [4]. G band represents the crystalline quality and is an evidence for the formation of hexagonal lattice in graphite. It is due to the sp^2 bond stretching of all pairs of carbon atoms. Single line appearing at 1580 cm^{-1} for monocrystalline graphite is highly symmetric [24].

The third prominent peak appears at 2670 cm^{-1} and is referred to as 2D peak/band. 2D band is the graphite like G band, which is a double resonance of D band [25].

In the case of Ni-7500 (Fig. 2e), an additional shoulder peak appears at 1610 cm^{-1} which

Table 1. Film deposition scheme.

Film nomenclature	Laser shots on Ni	Laser shots on graphite
Ni-3500	3500	200
Ni-4500	4500	200
Ni-5500	5500	200
Ni-6500	6500	200
Ni-7500	7500	200

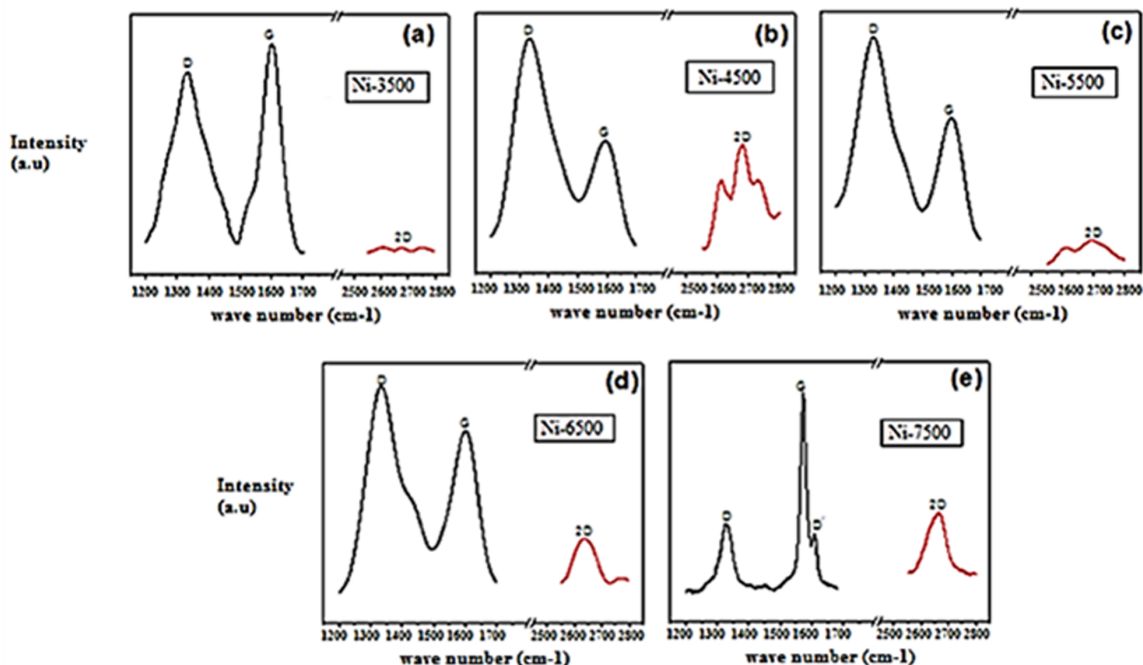


Fig. 2. Raman spectra of graphene prepared with different Ni concentrations which were varied by taking (a) Ni-3500, (b) Ni-4500, (c) Ni-5500, (d) Ni-6500 and (e) Ni-7500.

is referred to as D' peak (defected graphite). D and D' bands are indicative of defected graphite [23].

The main difference between the Raman spectra of graphene and graphite depends on the change in intensity, position and shape of 2D peak. 2D band can be used for determination of a number of graphene layers [25]. G and 2D bands position, width and shape can be changed by increasing the number of graphene layers [26]. The 2D band shown in Fig. 2(a-c) is splitted into two or three components which is due to armchair and zigzag orientation of the carbon atom sheet with respect to the strain axis [27].

The ratio I_D/I_G is used as a measure for non- sp^2 to sp^2 bonding and depends on the concentration of electrons. I_{2D}/I_G ratio is used to investigate the number of graphene layers. The intensities of I_D , I_G , I_{2D} and calculated ratios are given in Table 2.

An increase in I_D/I_G ratio in the Raman spectra of the films Ni-3500 and Ni-4500 shown in Fig. 2a and Fig. 2b indicates an increase in defects due to the large number of graphene layers. For Fig. 2(c-e), it is noticed that the intensity ratio of I_D/I_G appears to decrease with increasing laser shots on Ni target. Moreover, the Raman profile for Ni-7500 showing a significant decrease in D band intensity depicts the absence of defects.

Table 2. Raman intensities for I_D , I_G , I_{2D} , I_D/I_G and I_{2D}/I_G .

Sr. no.	Film	Intensity (a.u)			I_D/I_G	I_{2D}/I_G	Remarks
		I_D	I_G	I_{2D}			
1	Ni-3500	650	747	40	0.85	0.05	no graphene formation
2	Ni-4500	157	104	104	1.5	1	bi-layer graphene
3	Ni-5500	70	54	30	1.29	0.55	5 layer graphene
4	Ni-6500	130	112	65	1.16	0.58	4 layer graphene
5	Ni-7500	3179	5071	3115	0.62	0.65	tri-layer graphene

Changes in D, G and 2D peak positions in all films corresponding to different number of laser shots on Ni are illustrated in Table 3. In the case of Ni-7500, there is a shift in the D, G and 2D peak positions towards the lower wave numbers. A downward shift in 2D, D and G peak positions is also observed in the case of Ni-6500, Ni-5500 and Ni-4500, respectively. This downward shift is called red shift and is due to phonon softening, which is caused by tensile strain experienced by the layered structure [27]. Upward shift in D peak position of the film Ni-4500 and the shift in 2D peak positions of Ni-5500 and Ni-4500 towards the higher wave numbers are due to thermal stress, and they occur due to substrate heating. As a result of compressive stress, blue shifted 2D peak, due to phonon hardening, is observed in the Raman spectra [28].

In the case of Ni-3500 (Fig. 2a) the ratio I_{2D}/I_G is 0.05. Table 2 shows that there is no evidence of graphene formation. It means that 3500 number of laser shots on Ni is insufficient for the growth of graphene. The reason is that during laser ablation of the C target, the ejected C atoms are deposited on and adsorbed by the Ni layer. During substrate cooling, the amount of C segregated from Ni depends on the initial saturation status of C-Ni solid solution. For a fixed amount of C deposited onto the Ni films at 530 °C substrate temperature, C saturation in C-Ni solid solution is easier to reach the thinnest Ni film (Ni-3500). It results in the smallest Ni volume. Therefore, in this case, the sample reaches C supersaturation easily. When it is cooled to room temperature, the solubility of Ni becomes weak. Consequently, less carbon is required to form a solid solution with Ni films. The reduction of the solubility of Ni leads to C precipitation [29]. For

the deposited film Ni-4500, $I_{2D}/I_G = 1$, which gives the indication of bi-layer graphene [30]. The intensity of G peak increases linearly as the number of graphene layers increases [31]. In the case of films shown in Fig. 2 (c-e), the intensity ratios I_{2D}/I_G are more than 50 %, implying the formation of bi-, tri- and few-layer graphene [22].

In case of the film Ni-7500, the Raman spectrum (Fig. 2e) has a particular shape of 2D band, FWHM greater than 60 cm^{-1} and I_{2D}/I_G value < 1 , which all reveal the fact of existence of trilayer graphene. The film Ni-7500 also appears as the best film among all the deposited films, showing fewer defects (smallest I_D/I_G value) [32].

3.2. AFM analysis

AFM micrographs of the deposited films provide the detailed information about the surface morphology and the height of few-layer graphene by line profile. AFM in tapping mode has been used to characterize the samples.

Left column of Fig. 3 represents the 2D AFM micrographs of graphene deposited at different laser shots on Ni, keeping 200 laser shots on graphite constant for all deposition processes. Central column in Fig. 3 represents the corresponding line profile of the contrast image drawn at the intersection of layers along the lines indicated in the micrographs. Right column in Fig. 3 presents the 2D AFM micrographs after convolution process showing much clear, layer by layer, the growth of graphene.

The number of graphene layers can be identified by color contrast of images. The number of graphene layers can also be calculated

Table 3. Changes in D, G and 2D peak positions for different laser shots on Ni.

Film	Laser shots on Ni	D peak position	G peak position	2D peak position
Ni-3500	3500	1332	1600	2678
Ni-4500	4500	1334	1596	2680
Ni-5500	5500	1330	1600	2695
Ni-6500	6500	1332	1600	2635
Ni-7500	7500	1327	1571	2666

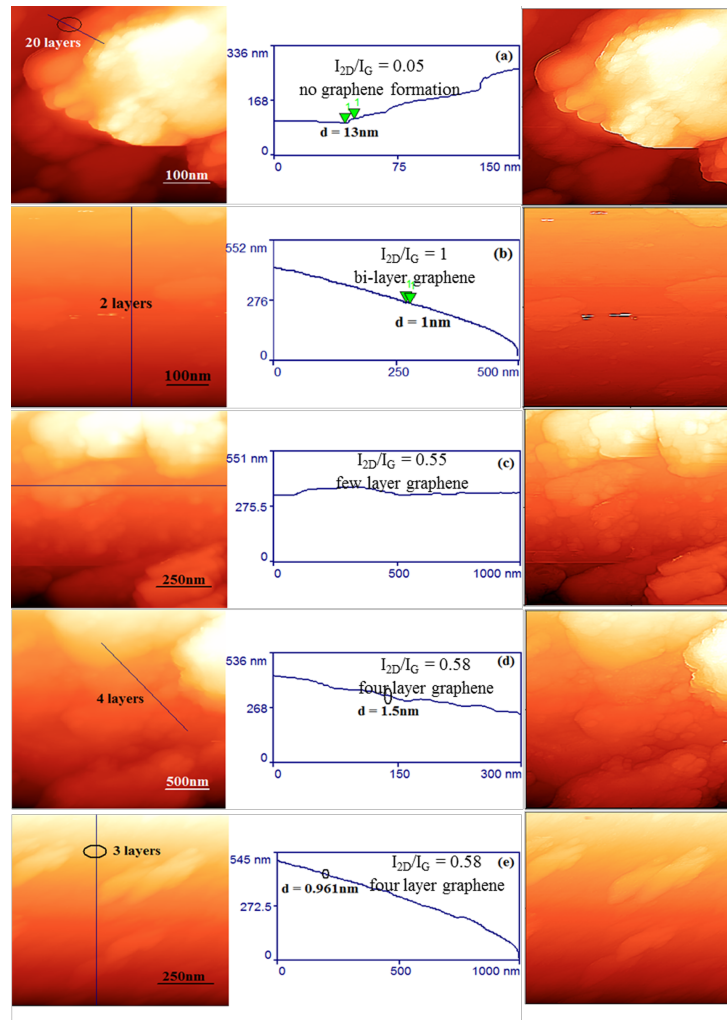


Fig. 3. AFM micrographs and line profiles of graphene prepared with different Ni concentration which was varied by using (a) 3500, (b) 4500, (c) 5500, (d) 6500 and (e) 7500 laser shots on Ni.

by using the formula $d_1 = n \times \Delta d$, where d_1 is the height of graphene layers, n is the number of layers and Δd is the theoretically measured value of interlayer spacing between two graphene layers, which is 0.335 nm [33].

The number of graphene layers equal to 38, calculated for the encircled region (thickness 13 nm) in the line profile of the AFM micrograph of Ni-3500 (Fig. 3a), gives a clear indication that there is no evidence of mono-, bi- or tri-layer

graphene formation. This result has also been verified by Raman spectra of the film Ni-3500. Bi-layer graphene is indicative in the region of 1 nm thickness, occurring in the line profile of Ni-4500 and Ni-5500.

The line profile of the sample Ni-6500 shown in Fig. 3d represents slight increase in graphene layers thickness ($d = 1.5$ nm) indicating 3 or 4 layers graphene formation [22].

For the film Ni-7500, the height profile across the vertical line marked on the AFM micrograph of Fig. 3e shows that the thickness of this graphene sample ranges from 0.9 nm to 1.2 nm, suggesting three graphene layers.

4. Conclusions

Optimized conditions for growing bi-, tri- and few layer graphene fabricated on Ni thin films were achieved by pulsed laser deposition technique. The growth conditions for Ni-7500 are the best to achieve low defect tri-layer graphene. 4500 number of laser shots on Ni has been proved as the best minimal Ni concentration to grow bi-layer graphene. Film Ni-3500 provides no indication of graphene growth due to nonuniform Ni matrix unable to grow graphene. It is concluded that graphene growth is sensitive to Ni film uniformity and concentration.

References

- [1] WALLACE P.R., *Phys. Rev.*, 71 (1947), 622.
- [2] NOVOSELOV K.S., GEIM A.K., MOROZOV S.V., JIANG D., ZHANG Y., DUBONOS V., *Science*, 306 (2004), 666.
- [3] GEIM A.K., NOVOSELOV K.S., *Nat. Mater.*, 6 (2007), 183.
- [4] DYCHALSKA A., POPIELARSKI P., FRANKOW W., FABISIAK K., PAPROCKI K., SZYBOWICZ M., *Mater. Sci-Poland*, 33 (2015), 799.
- [5] MERIC I., HAN M.Y., YOUNG A.F., OZYILMAZ B., KIM P., SHEPARD K.L., *Nat. Nanotechnol.*, 3 (2008), 654.
- [6] HAMILTON J.C., BLAKELY J.M., *Surf. Sci.*, 91 (1980), 199.
- [7] LYON H.B., SOMORJAI G.A., *J. Chem. Phys.*, 46 (1967), 2539.
- [8] ZHENG M., TAKEI K., HSIA B., FANG H., ZHANG X., FERRALIS N., KO H., CHUEH Y.L., ZHANG Y., MABOUDIAN R., JAVEY A., *Appl. Phys. Lett.*, 96 (2010), 063110.
- [9] NAST O., PUZZER T., KOSCHIER L.M., SPROUL A.B., WENHAM S.R., *Appl. Phys. Lett.*, 73 (1998), 3214.
- [10] TAN Z., HEALD S.M., RAPPOSCH M., BOULDIN C.E., WOICIK J.C., *Phys. Rev. B*, 46 (1992), 9505.
- [11] LI X., CAI W., AN J., KIM S., NAH J., YANG D., PINER R., VELAMAKANNI A., JUNG I., TUTUC E., BANERJEE S.K., COLOMBO L., RUOFF R.S., *Science*, 324 (2009), 1312.
- [12] REINA A., JIA X., HO J., NEZICH D., SON H., BULOVIC V., DRESSELHAUS M.S., KONG J., *Nano Lett.*, 9 (2009), 3087.
- [13] ZAROTTI F., GUPTA B., IACOPI F., SGARLATA A., TOMELLINI M., MOTTA N., *Carbon*, 98 (2016), 307.
- [14] CHO S.Y., KIM H.M., LEE M.H., LEE D.J., KIM K.B., *Curr. Appl. Phys.*, 12 (2012), 1088.
- [15] EDWARDS R.S., COLEMAN K.S., *Accounts Chem. Res.*, 46 (2013), 23.
- [16] STANKOVICH S., DIKIN D.A., PINER R.D., KOHLHAAS K.A., KLEINHAMMES A., JIA Y., WU Y., NGUYEN S.T., RUOFF R.S., *Carbon*, 45 (2007), 1558.
- [17] MOREAU E., FERRER F.J., VIGNAUD D., GODEY S., WALLART X., *Phys. Status Solidi A*, 207 (2010), 300.
- [18] AHMADI S., AFZALZADEH R., *Physica E*, 81 (2016), 302.
- [19] TITE T., DONNET C., LOIR A.-S., REYNAUD S., MICHALON J.-Y., VOCANSON F., GARRELIE F., *Appl. Phys. Lett.*, 104 (2014), 041912.
- [20] KOH A.T.T., FOONG Y.M., CHUA D.H.C., *Diam. Relat. Mater.*, 25 (2012), 98.
- [21] KUMAR I., KHARE A., *Appl. Surf. Sci.*, 317 (2014), 1004.
- [22] WANG K., TAI G., WONG K.H., LAU S.P., GUO W., *AIP Adv.*, 1 (2011), 022141.
- [23] FERRARI A.C., ROBERTSON J., *Phys. Rev. B*, 64 (2001), 075414.
- [24] TUINSTR A F., KOENIG J.L., *J. Chem. Phys.*, 53 (1970), 1126.
- [25] FERRARI A.C., *Solid State Commun.*, 143 (2007), 47.
- [26] FERRARI A.C., MEYER J.C., SCARDACI V., CASIRAGHI C., LAZZERI M., MAURI F., PISCANEC S., JIANG D., NOVOSELOV K.S., ROTH S., GEIM A.K., *Phys. Rev. Lett.*, 97 (2006), 187401.
- [27] HUANG M., YAN H., HEINZ T.F., HONE J., *Nano Lett.*, 10 (2010), 4074.
- [28] FERRALIS N., *J. Mater. Sci.*, 45 (2010), 5135.
- [29] WINTTERLIN J., BOCQUET M.L., *Surf. Sci.*, 603 (2009), 1841.
- [30] LU Y., MERCHANT C.A., DRNDI M., JOHNSON A.T.C., *Nano Lett.*, 11 (2011), 5184.
- [31] WANG Y.Y., NI Z.H., YU T., SHEN Z.X., WANG H.M., WU Y.H., CHEN W., WEE A.T.S., *J. Phys. Chem. C*, 112 (2008), 10637.

- [32] SEUNGHYUN L., KYUNGHOO L., ZHAOHUI Z.,
Nano Lett., 10 (2010), 4702.
- [33] NI Z.H., WANG H.M., KASIM J., FAN H.M., YU T.,
WU Y.H., FENG Y.P., SHEN Z.X., *Nano Lett.*, 7
(2007), 2758.

Received 2016-01-24
Accepted 2017-11-18